Operating Regimes of GaAs–AlGaAs Semiconductor Ring Lasers: Experiment and Model

M. Sorel, *Member, IEEE,* G. Giuliani, *Member, IEEE,* A. Scirè, *Member, IEEE,* R. Miglierina, *Student Member, IEEE,* S. Donati, *Fellow, IEEE,* and P. J. R. Laybourn

***Abstract*—Theory and experiments of single-mode ridge waveguide GaAs–AlGaAs semiconductor ring lasers are presented. The lasers are found to operate bidirectionally up to twice the threshold, where unidirectional operation starts. Bidirectional operation reveals that just above threshold, the lasers operate in a regime where the two counterpropagating modes are continuous wave. As the injected current is increased, a new regime appears where the intensities of the two counterpropagating modes undergo alternate sinusoidal oscillations with frequency in the tens of megahertz range. The regime with alternate oscillations was previously observed in ring lasers of the gas and dye type, and it is here reported and investigated in semiconductor ring lasers. A theoretical model based on a mean field approach for the two counterpropagating modes is proposed to study the semiconductor ring laser dynamics. Numerical results are in agreement with the regime sequence experimentally observed when the injected current is increased (i.e., bidirectional continuous-wave, bidirectional with alternate oscillations, unidirectional). The boundaries of the different regimes are studied as a function of the relevant parameters, which turn out to be the pump current and the conservative and dissipative scattering coefficients, responsible for an explicit linear coupling between the two counterpropagating field modes. By a fitting procedure, we obtain good numerical agreement between experiment and theory, and also an estimation for the otherwise unknown scattering parameters.**

***Index Terms*—Laser stability, optical bistability, optical scattering, ring lasers, scattering parameters measurement, semiconductor lasers.**

I. Introduction

SINCE THEIR first demonstration [1], semiconductor ring lasers (SRLs) have received increasing attention owing to their applications in photonic integrated circuits. They do not require cleaved facets or gratings for optical feedback and thus are particularly suited for monolithic integration. They are promising candidates for wavelength filtering, unidirectional travelling-wave operation, and multiplexing/demultiplexing applications.

Several examples of fabrication and characterization of SRLs have been reported. Different cavity geometries have been proposed, such as circular [2], [3], racetrack [4], [5], square [6], [7], and triangular [8], employing various light-guiding mechanisms such as pillbox structures using the "whispering-gallery" effect [2], deep-etched or rib-waveguides [3], [4], shallow-etched ridge waveguides [9], buried heterostructures [10], and recently photonic-wire microcavities [11]. An important feature of the design of such devices is the output coupler, which profoundly influences the operating characteristics of the laser. Advantages and limitations of evanescent coupling, Y-junction, and multimode interference (MMI) couplers have been analyzed in great detail [12], [13]. Some monolithic SRLs exhibited unidirectional operation [5], [14], [15] which is highly desirable to improve the device performances, and can lead to bistability [16], with the prospect of application in systems for all-optical switching, gating, wavelength-conversion functions, and optical memories.

Besides the several SRL geometries fabricated, different theoretical models have been proposed for the analysis of generalized rings and two-mode laser systems. The theories focus on a study of the interplay between the two counter-propagating modes and their interaction with the active medium. The most widely studied system is the He-Ne ring laser [17], because of the interest raised by the demonstration of the optical gyroscope. A particular treatment was devised for the SRL by Sargent *et al*. [18], who derived a simple model for the intensities of the two modes starting from first principles, enlightening the importance of the self- and cross-gain saturation parameters. Later, Mandel *et al.* [19] proposed a model for the electric field, also accounting for the carrier induced grating dynamic, which better applies to a configuration with two co-propagating modes. However, a comparison between experimental results in SRL and a suitable theoretical explanation has not yet been carried out systematically.

In this paper, we report on the fabrication, characterization, and modeling of single lateral-mode SRLs. The devices are large radius ring cavities weakly coupled to a straight output waveguide, fabricated in the GaAs–AlGaAs material system. Bidirectional and unidirectional regimes with continuous-wave mode operation have been experimentally observed. In addition, we have also measured a new bidirectional regime where the two counterpropagating modes undergo harmonic alternate oscillations. The latter regime was previously observed in ring lasers of the gas [20] and dye type [21], and we reported it for the first time in SRLs [22]. The results have been described within a theoretical framework based on two mean-field equations for the counterpropagating modes, and on a third rate equation for the carriers. The model accounting for self and cross-gain saturation effects and backscattering contributions

Manuscript received June 20, 2002. The work of M. Sorel and A. Scirè was supported by the European Union under Marie Curie Fellowship Contracts HPMF-CT-1999-00083 and HPMF-CT-2000-00617.

M. Sorel and P. J. R. Laybourn are with the Department of Electronics and Electrical Engineering, University of Glasgow, Glasgow G12 8QQ, U.K.

G. Giuliani, R. Miglierina, and S. Donati are with the Dipartimento di Elettronica, Università di Pavia, I-27100 Pavia, Italy.

A. Scirè is with the Instituto Mediterraneo de Estudios Avanzados, CSIC-UIB, Campus UIB, E-07071 Palma de Mallorca, Spain.

Digital Object Identifier 10.1109/JQE.2003.817585

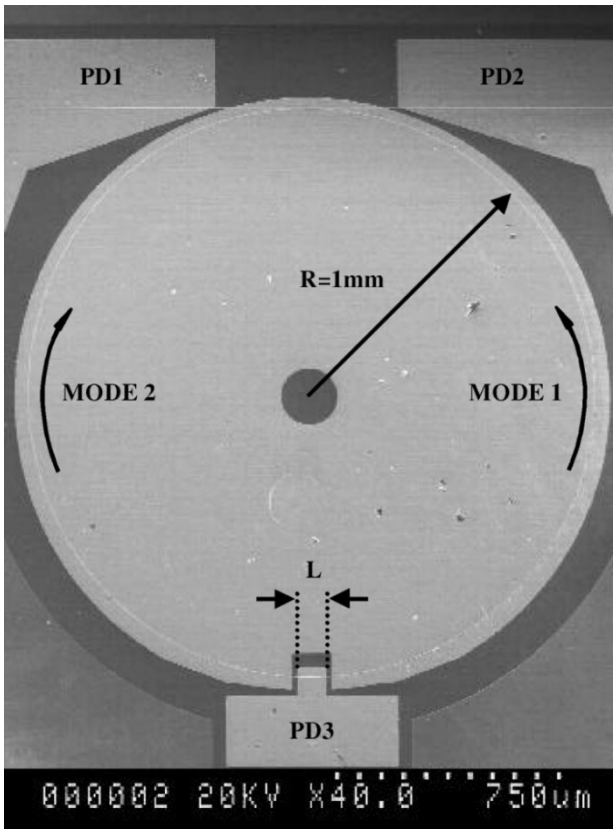

Fig. 1. (a) Micrograph of the device showing the contact layout with the ring biasing contact and the three integrated photodetectors. (b) Schematic cross section of the waveguide where d represents the etching depth.

is suitable for describing the device behavior. The dynamics of the alternate oscillation regime have been investigated in detail, and a self-consistent fitting procedure has yielded a quantitative agreement between calculated and experimental waveforms.

II. Device Design and Fabrication

A SEM micrograph of the devices, with the layout of the ohmic contacts made to the structure, is shown in Fig. 1(a). The lasers are 1-mm-radius ring cavities evanescently coupled to a straight output waveguide. The gap between the laser cavity and the output waveguide is 1 μm, providing a theoretical evanescent coupling of 1%–5% depending on the etching depth of the waveguides. In order to focus the analysis on the intrinsic operating regimes of the SRL and on the interaction between the two counterpropagating modes, the output waveguide is tilted at 5° to the cleaved faces of the substrate to reduce the optical back reflection to <0.5%. Two separate contacts were deposited at each end of the straight output waveguide, acting as integrated photodetectors and providing further reduction of the backreflection when reverse-biased. The length of each contact is 800 μm, leaving an unpumped waveguide section of 50 μm beside the directional coupler. In order to monitor the total light intensity within the ring, an in-line photodetector was fabricated by defining a separately biased section along the ring, ranging from 50 to 200 μm long, with a 10-μm separation to the main ring biasing contact. To assess the influence of residual backreflection from the output waveguides on the different measured laser regimes, some ring cavities were fabricated without any output waveguide. In Section III, it will be shown that the influence of the residual backreflections from the output waveguides is negligible.

The devices were fabricated in standard double-quantum-well (DQW) GaAs–AlGaAs material grown at Sheffield University by MOCVD. The active region has a GaAs double quantum well sandwiched between two $Al_{0.2}Ga_{0.8}As$ waveguide regions, each 250 nm thick. The p-type and n-type cladding layers consist of 1.0- and 1.5-μm-thick $Al_{0.4}Ga_{0.6}As$, respectively. Highly p-doped GaAs 100-nm-thick is used as a contact layer. A transverse section of the waveguide is depicted in Fig. 1(b).

For reasons of flexibility, the devices were fabricated by electron-beam lithography. However, the waveguide and coupler dimensions are not critical, and standard optical lithography provides equally accurate results. For the fabrication of the waveguides, we designed a shallow-etched ridge geometry that ensures operation on a single-transverse mode. The waveguide width is 2 μm, defined by $SiCl_4$ reactive ion etching. The electrical insulation is provided by a 300-nm-thick layer of PECVD SiO_2 and the ohmic contacts consist of Ti/Pd/Au and Ti/Ge/Au for the p- and n-type respectively. The etching depth d [also shown in Fig. 1(b)] is the most critical parameter in the fabrication process because of its impact on the bending and the scattering losses. Accurate control of this parameter was performed by using *in situ* reflectometry during dry etching [23]. Smaller radius SRLs are more appealing for monolithic integration but require higher waveguide confinement to minimize bending losses. A large radius device provides more flexibility in the waveguide etched depth, allowing a comparative analysis of the influence of the waveguide sidewall scattering on the laser threshold and on the output regimes.

III. Experiment

All fabricated SRL devices were tested by injecting a dc forward current into the ring contact, with the heat-sink kept at 25 °C constant temperature. Three electrical probes were used for reverse-biasing the three photodiodes PD1, PD2, and PD3 [see Fig. 1(a)], from which photocurrents were measured by means of transimpedance amplifiers. The insulation resistance between the ring contact and the in-line photodiode (PD3) and the waveguide photodiodes (PD1 and PD 2) were typically 5–10 and 20–50 kΩ, respectively. More than 90% of the fabricated devices exhibited lasing action, with threshold currents varying

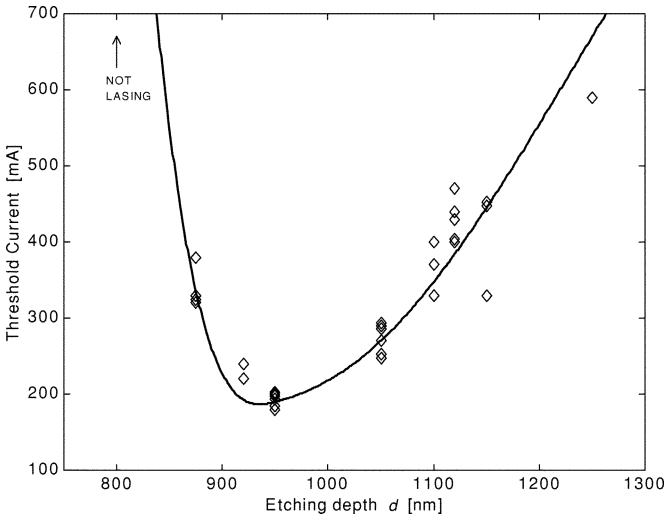

Fig. 2. Plot of experimentally measured threshold currents for 32 fabricated SRL devices as a function of the etching depth d. Injected current is dc. Temperature is 25 °C. Ring radius is 1 mm. The solid line is drawn for visual interpolation purposes.

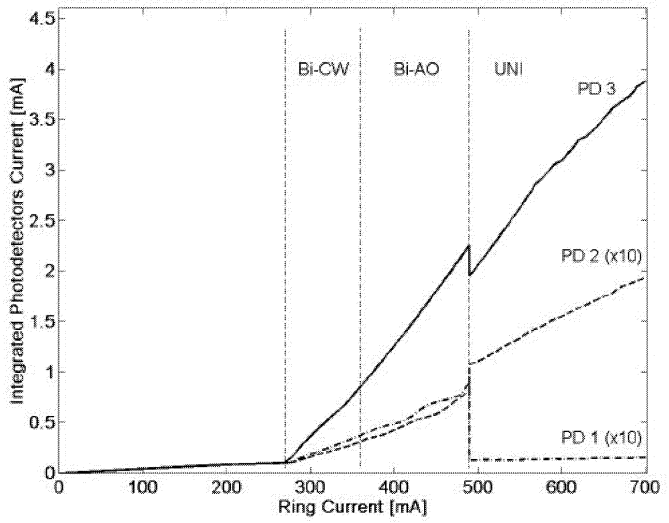

Fig. 3. Experimental *L–I* characteristics of sample SRL device. One curve is depicted for each integrated photodetector. PD3 is the in-line photodiode. PD1 and PD2 are output waveguide photodiodes that detect the power of mode 1 (anti-clockwise) and mode 2 (clockwise). Photocurrents from PD1 and PD2 are multiplied by a factor 10. The ring current intervals for the three different operating regimes (bidirectional-CW, bidirectional with alternate oscillations, unidirectional) are also shown.

from 190 to 600 mA. Fig. 2 reports the measured threshold currents for 32 fabricated devices as a function of the etching depth d of the ridge [see Fig. 1(b)]. A minimum of the current threshold is achieved for $d = 950\ \mathrm{nm}$, which corresponds to an upper cladding thickness of 50 nm. Shallower etching depths cause an increase of waveguide bending losses, and deeper etching increases the amount of loss due to light scattering by ridge sidewalls roughness. The minimum threshold value of 190 mA corresponds to a current density of $1.51\ \mathrm{kA/cm^2}$.

The *L–I* curves obtained from the three integrated photodiodes (PD3 biased at 0 V; PD1 and PD2 reverse biased at -1.5 V) for a sample device with etching depth $d = 1050\ \mathrm{nm}$, in-line photodiode length of 200 $\mu\mathrm{m}$ and a threshold of 270 mA are reported in Fig. 3. Photocurrents from PD1 and PD2 are, respectively, a direct measure of the power of mode 1 (counter-clockwise) and mode 2 (clockwise). As long as dc values of the photodetected currents were considered, two distinct operating zones could be identified. In the first zone (from threshold to 480 mA), bidirectional laser operation occurred, i.e., the two modes were both active. In the second zone (above 480 mA), the laser operated unidirectionally on mode 2. The transition from bidirectional to unidirectional operation is abrupt. Repeated measurements showed that, occasionally, at the onset of SRL unidirectional operation mode 1 becomes active instead of mode 2.

Optical spectra from the two output waveguides 1 and 2 were taken using a grating-based optical spectrum analyzer (OSA) and a scanning Fabry–Perot filter with 300-GHz free spectral range (FSR). The latter measurement revealed that SRL devices operated on a single longitudinal mode. Simultaneous OSA measurements revealed that in bidirectional operation the wavelengths of modes 1 and 2 were the same (e.g., 860 nm), at least within the OSA repeatability of 0.005 nm. As the latter value corresponds to about 0.15 of the SRL free spectral range (13.4 GHz or 0.034 nm), it can be concluded that, when bidirectional operation occurs, counterpropagating modes 1 and 2 are locked to the same wavelength. When the in-line photodetector PD3 was strongly reverse-biased, and large CW current values (close to 700 mA) were injected into the ring, modelocking operation of the SRL was observed, as is typical for these structures [24].

Further measurements were carried out to gain understanding of the SRL bidirectional operation. By contacting the integrated photodiodes with radio frequency (RF) electrical probes, it was found that bidirectional operation did not always occur with the counterpropagating modes 1 and 2 in continuous wave. Rather, a new regime was observed in which modes 1 and 2 underwent alternate amplitude harmonic oscillations. As illustrated by the vertical dashed lines of Fig. 3, three distinct operating regimes of the SRL can be identified for varying injected current. The first regime occurs from threshold up to 360 mA, and exhibits the two modes 1 and 2 operating in continuous wave. This first regime is called *bidirectional continuous wave* (bi-CW). In the second regime, occurring from 360 to 480 mA, the intensities of the two counterpropagating modes 1 and 2 are modulated by harmonic sinusoidal oscillations, the modulation being alternate, or out-of-phase, for the two modes; i.e., when mode 1 has a maximum intensity, mode 2 has a minimum. We call this second regime *bidirectional with alternate oscillations* (bi-AO). In the third regime, occurring above 480 mA, one of the two modes is suppressed, and all the lasing power is provided to the other mode alone which operates CW. We call this third regime *unidirectional* (UNI).

Evidence of the new bi-AO regime was found by simultaneously displaying the waveforms of the currents detected by waveguide photodiodes 1 and 2 on a 50 Ω input oscilloscope. A typical example of such a measurement is reported in Fig. 4(a), where it can be noted that the intensities of modes 1 and 2 are sinusoidally modulated at the frequency of 110 MHz and they are out-of-phase. The modulation depth of the waveforms is defined as $\mathrm{MD_n} = \Delta I_\mathrm{n}/I_\mathrm{dc,n}$, where ΔI_n is the amplitude of the sine photocurrent term, $I_\mathrm{dc,n}$ is the dc photocurrent value and the suffix $\mathrm{n} = 1, 2$. For the case reported in Fig. 4(a), we have $\mathrm{MD_1} \approx \mathrm{MD_2} \approx 0.5$. Fig. 4(b) reports the electrical spec-

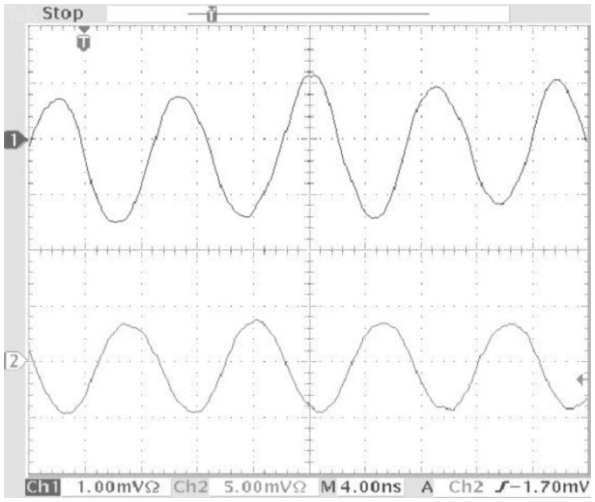

(a)

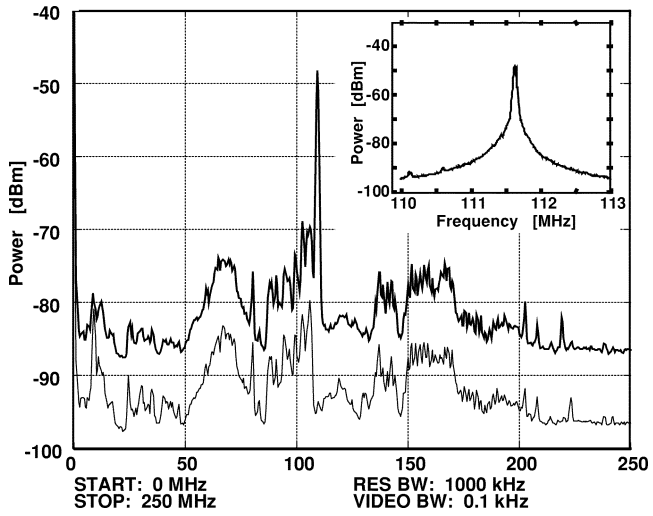

(b)

Fig. 4. (a) Experimental time traces of the intensities of modes 1 and 2 in the bidirectional regime with alternate oscillations. The RF component of the photocurrents generated by photodiodes PD1 and PD2 are displayed on a 50 Ω input digital oscilloscope. The intensities are sinusoidally modulated at 110 MHz, and are out-of-phase. The dc current injected into the ring laser is 380 mA, and photodiodes PD1 and PD2 are reverse biased at −1.5 V. (b) Thick trace: RF spectrum of the photocurrent generated by PD1 for the same conditions of case (a). The peak of the alternate oscillation at 110 MHz is visible, as well as a small second harmonic component. Thin trace: spectrum measured with the laser switched off (offset by −10 dB for clarity), showing background noise and disturbances. The inset shows a detailed spectrum of the AO, measured with a 30-kHz resolution bandwidth.

trum of the photocurrent detected by PD1 in the bi-AO regime, showing a peak at 110 MHz. Higher resolution measurement shown in the inset of Fig. 4(b) revealed that the linewidth of the oscillations amounts to 50 kHz. Periodic waveforms were also observed from the contact of the in-line integrated photodiode PD3; they will be discussed in more detail in Section IV after the theoretical analysis is presented.

For the sample SRL device described here, the frequency of the alternate oscillations at the onset of the bi-AO regime was 115 MHz and as the ring laser current was increased, the oscillation frequency decreased almost linearly. Corresponding with the upper limit of the bi-AO regime the oscillation frequency was 80 MHz. When the device was operated close to the upper limit of the bi-AO regime, the oscillations of the mode intensities became distorted, resembling triangular waveforms, and higher harmonics appeared in the RF spectrum. These features are reported later in Figs. 6 and 7, and they will be illustrated in Section IV.

For a specific device, the sequence of the three regimes identified above occurred with good repeatability. When the injected ring current was set to the maximum value of 700 mA and subsequently decreased, the transitions between the three regimes showed some hysteresis, which approximately amounted to 15% of the ring current value. The behavior described above was common to almost all the fabricated devices. The measured values for the frequency of the alternate oscillations at the onset of the bi-AO regime showed spreading in the 50–140 MHz range from device to device, and the trend of decreasing frequency of the alternate oscillations for increasing injected ring current was reported in all devices. The modulation depths MD_n varied from a few percent to 50%. In the UNI regime, some devices exhibited repeated switching between mode 1 and mode 2 when injected current was increased, in a manner similar to that reported in [16]. The switching behavior of the devices in the UNI regime is not further analyzed in the present work. Devices with different etching depths displayed some differences in the behavior. In particular, deeper etched ridge SRLs showed a reduction of the extension of the bi-AO regime, or even its suppression, mostly in favor of the UNI regime. As will be explained in Section IV, this different behavior may be caused by increased scattering from the ridge sidewall roughness.

To confirm the general trends presented above, some different device configurations were designed, fabricated and tested. Among these, SRL devices identical to that depicted in Fig. 1(a), except for the absence of the output waveguide, served to verify that the observed regimes were not caused by, or strictly dependent on, the presence of the output waveguide, which could provide the ring laser with feedback from the end chip facets. In these devices, bidirectional and unidirectional operation were discerned by collecting the radiated lasing light of modes 1 and 2 lost by curvature with two multi-mode fibers placed outside the laser chip, and the bi-AO regime could be observed by measuring the RF modulation appearing in the photocurrent generated by the in-line photodiode (PD3). The RF signal measured from PD3 for the devices without the output waveguide was similar to that measured for the devices with the output waveguide. In some measurements, the in-line photodiode PD3 was forward-biased with a current density equal to that of the laser ring, so as to reduce perturbations in the ring cavity to a minimum. Again, the bi-AO regime could still be observed by looking at the RF voltage signal of the forward-biased photodiode PD3, used as transparent detector [25], and the reported dependence of the frequency of the alternate oscillations on the injected ring current was the same as that obtained when the detector was reverse-biased.

From these additional experimental results, it is concluded that the occurrence of the three distinct operating regimes (bi-CW, bi-AO, UNI) in index-guided SRLs is an intrinsic feature of single-mode ring semiconductor lasers, and is not mainly caused by feedback effects external to the ring.

IV. Model

In this section, we model the semiconductor ring laser to carry out numerical simulations to illustrate the different operating regimes, and to fit the unknown parameters.

In single longitudinal mode operation, the electric field inside the ring cavity can be expressed as

$$E(x,t) = E_1(t)e^{-i(\Omega t - kx)} + E_2(t)e^{-i(\Omega t + kx)} \tag{1}$$

where E_1 and E_2 are the mean-field slowly varying complex amplitudes of the electric field associated with the two propagation directions, i.e., mode 1 (counter clockwise) and mode 2 (clockwise) respectively; x is the spatial coordinate along the ring, assumed positive in the counter clockwise direction, and Ω is optical frequency of the selected longitudinal mode. The time evolution of the fields can be described by the following set of equations:

$$\frac{dE_{1,2}}{dt} = \frac{1}{2}(1+i\alpha)\cdot\left[G_{1,2}(N,E_{1,2}) - \frac{1}{\tau_{\rm p}}\right] \cdot E_{1,2} - K\cdot E_{2,1} \tag{2}$$

$$G_{1,2}(N,E_{1,2}) = G_{\rm n}(N-N_0) \cdot \left(1 - \varepsilon_{\rm s}|E_{1,2}|^2 - \varepsilon_{\rm c}|E_{2,1}|^2\right) \tag{3}$$

where α is the linewidth enhancement factor accounting for phase-amplitude coupling in the semiconductor medium, $G_{1,2}$ is the modal gain factor for the two modes, depending on the semiconductor gain factor $G_{\rm n}$, on the carrier density N, on the carrier density at transparency N_0 and on the field intensities $|E_1|^2$ and $|E_2|^2$ through nonlinear saturation effects. The self- and cross-gain saturation coefficients are given by ε_s and $\varepsilon_{\rm c}$, respectively and the photon lifetime in the ring cavity is $\tau_{\rm p}$. The parameter $K = K_{\rm d} + iK_{\rm c}$ represents an explicit linear coupling rate between the two modes. As the standing-wave pattern has a spatial period much smaller than carrier diffusion length, longitudinal variations of the carrier density can be neglected [19], and for the uniform carrier density N, the following equation holds:

$$\frac{dN}{dt} = \frac{J}{el} - \frac{N}{\tau_{\rm s}} - G_1(N,E_{1,2})\cdot|E_1|^2 - G_2(N,\text{Å}_{1,2})\cdot|E_2|^2 \tag{4}$$

where J is the injected ring current density, e is the electron charge, l is the active layer thickness, and $\tau_{\rm s}$ is the carrier lifetime.

Our model parallels that proposed by Numai for a semiconductor ring laser [26], except for the fact that we neglect spontaneous emission and we explicitly write the equations in terms of complex fields, thus accounting for phase effects.

An explicit coupling between the two counterpropagating fields is added through the backscattering rate $K = K_d + iK_{\rm c}$, which indicates the complex fraction of $E_{1(2)}$ that is injected in $E_{2(1)}$, per time unit. According to previous literature, $K_{\rm d}$ represents the dissipative coupling and $K_{\rm c}$ represents the conservative coupling [27]. The actual value for K in a SRL is determined by localized and distributed variations of refractive index and loss of the passive ring cavity [20]. In our model, $K_{\rm d}$ and $K_{\rm c}$ are regarded as fitting parameters, and their values will be estimated through a comparison with the experimental SRL regimes.

Equations (2)–(4) can be suitably rescaled, leading to the following dimensionless set:

$$\frac{{\rm d}E_{1,2}}{dT} = (1+i\alpha)\cdot[\xi_{1,2}n - 1]\cdot E_{1,2} - (k_{\rm d} + ik_{\rm c})\cdot E_{2,1} \tag{5}$$

$$\frac{dn}{dT} = 2\gamma\cdot\left[\mu - n\cdot\left(1 - \xi_1|E_1|^2 - \xi_2|E_2|^2\right)\right] \tag{6}$$

$$\xi_{1,2} = 1 - s|E_{1,2}|^2 - c|E_{2,1}|^2 \tag{7}$$

where the symbols E_1 and E_2 indicate the new counterpropagating fields. The new normalized variables and parameters are defined as follows:

$$T = \frac{t}{2\tau_{\rm p}};\quad E_{1,2} = \sqrt{G_{\rm n}\tau_{\rm s}}\cdot E_{1,2};\quad n = G_{\rm n}(N-N_0)\cdot\tau_{\rm p}$$

$$s = \frac{\varepsilon_{\rm s}}{G_{\rm n}\tau_{\rm s}};\quad c = \frac{\varepsilon_{\rm c}}{G_{\rm n}\tau_{\rm s}};\quad k_{\rm d} = 2\tau_{\rm p}\cdot K_{\rm d};\quad k_{\rm c} = 2\tau_{\rm p}\cdot K_{\rm c}$$

$$\gamma = \frac{\tau_{\rm p}}{\tau_{\rm s}};\quad \mu = \frac{J - J_0}{J_{\rm TH} - J_0}.$$

T represents the dimensionless time scale, s and c are normalized self- and cross-gain saturation coefficients, $k_{\rm d}$ and $k_{\rm c}$ are dissipative and conservative scattering coefficients, μ is the pump parameter, defined as a function of the actual injected current density J and of the threshold and transparency current densities, which are respectively given by

$$J_{\rm TH} = \frac{ed}{\tau_{\rm s}}\left(N_0 + \frac{1}{G_{\rm n}\tau_{\rm p}}\right);\quad J_0 = \frac{ed}{\tau_{\rm s}}\cdot N_0.$$

The laser threshold condition corresponds to $\mu = 1$. The rescaled set (5)–(7) allows us to focus directly on the parameters that actually influence the dynamics.

The set of (5)–(7) describes all the significant dynamics encountered in the experiments. In particular, an analytical study of the set (5)–(7) can be performed, supplying some interesting results concerning the SRL dynamics in the bi-AO regime [22]. However, here we choose to analyze the SRL behavior by numerically solving the set (5)–(7) through a standard Runge–Kutta integration algorithm. As a result, the different SRL operating regimes are found, as well as their dependence on scattering parameters $k_{\rm d}$ and $k_{\rm c}$ and on the pump factor μ. Other parameters are assigned a fixed value, i.e., $\alpha = 3.5$ and $\tau_{\rm s} = 1$ ns. A typical value $\tau_{\rm p} = 10$ ps was obtained from waveguide loss measurements, which is about a factor of 5–10 larger than the usual value for cleaved-facet linear cavity semiconductor lasers, due to the low output coupling and the long cavity length of the SRL. A value of 0.55 $\rm kA/cm^2$ was measured for the transparency current density J_0 by injecting externally modulated light into the straight output waveguide, and by determining the forward current bias of the terminal waveguide section that provided a sign reversal for the voltage signal measured at the contact [25]. The quantity of interest is the ratio $J_0/J_{\rm TH}$ that appears in the expression for the pump factor μ; the measured value was $J_0/J_{\rm TH} = 0.26$ for the sample device.

Numerical results show that, as long as the condition $\gamma \ll 1$ is fulfilled, the SRL regimes and dynamics only weakly depend on γ. This means that the time-scale evolution of the carriers

is much shorter than that of the alternate oscillations, and the carriers adiabatically follow the dynamics of the field. In our case $\gamma = 0.01$, and the above consideration holds. The calculated qualitative SRL behavior does not depend on the values of c and s, provided the condition $c > s$ is fulfilled. The condition $c > s$ was reported for different ring laser systems, and a detailed analysis based on Maxwell–Bloch equations showed that for two resonant modes in a ring cavity $c = 2s$ [28].

When the set of (5)–(7) is solved for increasing values of the pump coefficient μ, the sequence of calculated SRL regimes coincides with that reported in the experiments: a bi-CW regime occurs just above threshold, followed by the bi-AO regime and finally by the UNI regime. In the calculated bi-CW regime, the two counterpropagating modes operate CW and have the same intensity. In the calculated bi-AO regime, the intensities of the two modes are sinusoidally modulated and are out of phase. For higher pump values, the bidirectional regime with alternate oscillations becomes unstable and unidirectional operation is obtained. As (6) indicates, the active mode lasing in the unidirectional regime can be either of the two, depending on initial conditions.

A graphical representation of the calculated operating zones for the SRL is shown in Fig. 5(a), which depicts the boundaries of the three regimes (bi-CW, bi-AO, and UNI) in the plane μ (pump factor)—k_{d} (dissipative scattering coefficient), regarding the conservative scattering coefficient k_{c} as a parameter. For smaller k_{d} values, the regime sequence observed when the pump factor (i.e. ring laser current) is increased corresponds to the one experimentally reported: bi-CW, bi-AO, UNI. An increase in the value of the conservative scattering coefficient k_{c} enlarges the extension of the bi-CW region toward higher pump factors. Conversely, an increase in the value of the dissipative scattering coefficient k_{d} narrows the bi-AO region, which may even disappear if k_{d} is further increased, so that a direct transition between the bi-CW regime and the UNI regime occurs. It appears that the occurrence of bidirectional operation with alternate oscillations is favored by conservative scattering, and is hindered by dissipative scattering. This assertion is reinforced by the graph of Fig. 5(b), showing the boundaries of the three different SRL regimes in the plane $k_{\mathrm{d}} - k_{\mathrm{c}}$ for a pump factor $\mu = 2.15$. For the bi-AO regime, contour lines for the calculated frequency of the alternate oscillations are also plotted. Again, it can be argued that in order for the alternate oscillations to take place, a sufficiently small value of the dissipative scattering coefficient k_{d} is required, together with a sufficiently large value of the conservative scattering coefficient k_{c}. The frequency of the alternate oscillations increases for increasing k_{c}, while it decreases for increasing k_{d}. In summary, it appears that conservative scattering acts as a driving force for the alternate oscillations, while dissipative scattering tends to restore CW operation, either bidirectional or unidirectional depending on the value of the conservative scattering.

After the general description of the different SRL operating regimes was derived using the proposed model, an attempt was made to find a more quantitative agreement between experimental and theoretical results, following a suitable fitting procedure. Our goal is to estimate the values of the dissipative and

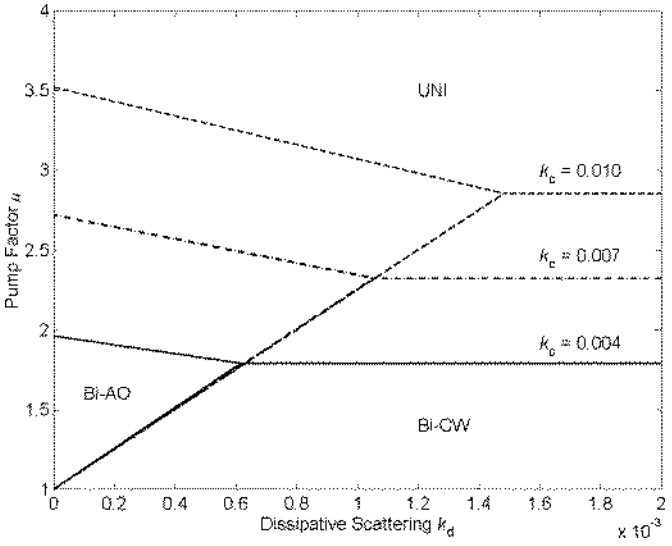

(a)

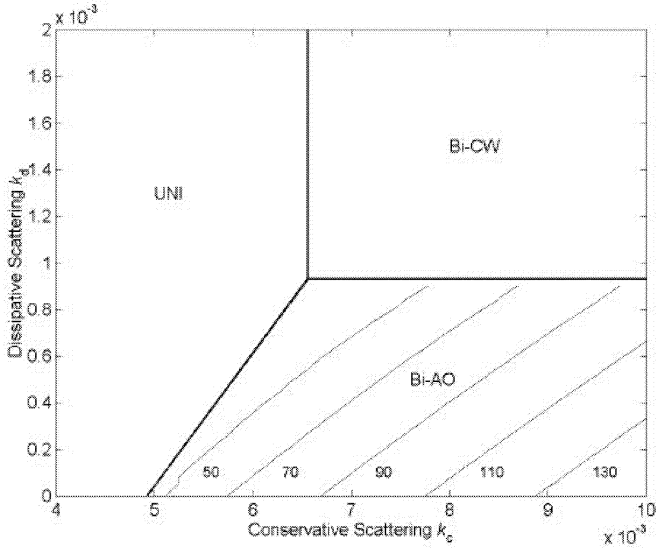

(b)

Fig. 5. Numerical simulation results illustrating the occurrence of the three different SRL regimes (bidirectional-CW, bidirectional with alternate oscillations, unidirectional). (a) Diagram for the plane μ (pump factor) versus k_{d} (dissipative scattering coefficient), for three different values of k_{c} (conservative scattering coefficient) reported on the graph; the extension of the bi-AO regime increases for larger k_{c} values. (b) Diagram for the plane k_{d} (dissipative scattering coefficient) versus k_{c} (conservative scattering coefficient) calculated for a pump factor $\mu = 2.15$, reporting also level curves for the frequency of alternate oscillations in the bi-AO regime. Values of other parameters, common to the two diagrams are: $\tau_{\mathrm{s}} = 1$ ns; $\tau_{\mathrm{p}} = 10$ ps; $\mathrm{s} = 0.003$; $\mathrm{c} = 0.006$; $\alpha = 3.5$.

conservative scattering coefficients, which can be computed explicitly in the case of gas ring lasers [27], but have never been investigated in semiconductor ring lasers.

As reported in Section III, for all the SRL devices that exhibited bidirectional operation with alternate oscillations, the measured frequency of the oscillations always decreased for increasing injected ring current. The purpose of the fitting procedure is to provide appropriate values for the scattering coefficients k_{d} and k_{c}, so that the calculated dependence of the alternate oscillations frequency versus the pump factor matches experimental results.

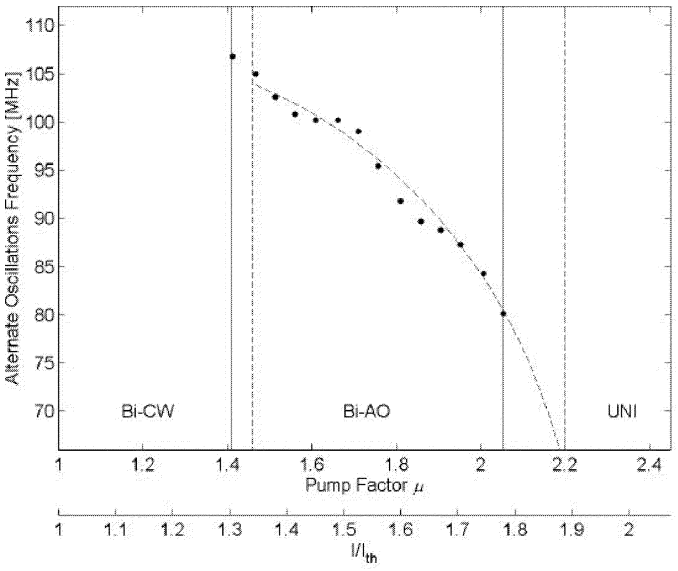

Fig. 6. Graph reporting the experimental and calculated dependence of the frequency of alternate oscillations versus ring laser current (or, equivalently, the pump factor μ). Dots are obtained from experimental measurements performed on the sample SRL device. The dashed curve is obtained from numerical solution of the theoretical SRL model, using the parameters yielded by the fitting procedure described in Section IV, i.e., $k_{\rm d} = 0.46\ 10^{-3}$; $k_{\rm c} = 8.5\ 10^{-3}$; $c = 2s = 9.3\ 10^{-3}$. Vertical lines represent the boundaries of the bidirectional regime with alternate oscillations, as obtained from experiment (solid lines) and theory (dashed lines).

A starting point for the fitting procedure for a particular SRL device is to measure the onsets of its various regimes and the frequency of the alternate oscillation as a function of the injected ring current, which is reported in Fig. 6 (full circles). By using appropriate theoretical analytical expressions for the alternate oscillation frequency appearing at the onset of the bi-AO regime and for the extension of the bi-AO region [22], estimated values for $k_{\rm d}$ and $k_{\rm c}$ are obtained. Subsequently, the value for the self-gain saturation coefficient s is slightly adjusted, so as to make the calculated transition pump values coincide with those reported experimentally. The fitting procedure performed for the sample device yielded the following values: $k_{\rm d} = 0.46\ 10^{-3}$; $k_{\rm c} = 8.5\ 10^{-3}$; $c = 2s = 9.3\ 10^{-3}$. The corresponding value for the nonnormalized self-gain saturation coefficient is $\varepsilon_{\rm s} = 2.7 \cdot 10^{-18}\ {\rm cm}^3$, in agreement with a typical value reported in the literature [29]. Numerical results obtained for the frequency of alternate oscillations are reported in Fig. 6 with the dashed line. Good agreement between theory and experiment is found.

Good agreement is also obtained between experimental and calculated time evolution of mode intensities, which are depicted in Fig. 7. Fig. 7(a) and (b) reports measured and calculated time waveforms for the intensities of the two counterpropagating modes for an injected ring current of 380 mA, corresponding to $\mu = 1.55$. Fig. 7(c) and (d) reports experimental and calculated results for an injected ring current of 440 mA, corresponding to $\mu = 1.85$, i.e., a pump value close to the upper boundary of the bi-AO region. The lower traces of Fig. 7(c) and (d) report the waveforms for the intensity of mode 1. The intensity oscillations of mode 1 are no longer purely sinusoidal; rather, higher harmonics are starting to appear in the modulating waveform. The same behavior is observed for mode 2. A possible interpretation for the occurrence of this waveform distortion lies in the fact that when the pump factor is increased, and hence the field intensifies, there is an increase of nonlinear mode coupling through cross-gain saturation. This nonlinear coupling perturbs the system dynamics and favors unidirectional continuous-wave operation, thus competing with the linear conservative coupling that acts as the driving force for the oscillations. Finally, the upper traces of Fig. 7(c) and (d) report measured and calculated waveforms for the photocurrent generated by the in-line photodiode (PD3) for the same injected ring current of 440 mA. The photocurrent generated by PD3 is a measure of the total optical power below the contact. When alternate oscillations are mostly harmonic, the in-line photodiode is expected to measure no RF signal. Actually, a small RF signal is always measured, because: 1) slight ring laser asymmetries (such as localized defects and nonhomogeneousity of ring pump current density) make the actual intensities of modes 1 and 2 different in correspondence with the position of the in-line photodiode; 2) unavoidable higher harmonics of the oscillation are detected. Fig. 7(c) and (d) report a case where higher harmonic components are relevant, and a distorted waveform is observed.

V. Conclusions

Systematic and complete investigations have been carried out on the lasing operating regimes of GaAs–AlGaAs single-mode SRLs. It is shown that, for increasing injecting current values, the devices exhibit a transition from bidirectional to unidirectional operation. A more accurate analysis of the dynamics of the SRLs revealed the existence of a new interesting operating regime where the two counterpropagating modes undergo sinusoidal alternate oscillations at frequencies in the tens of megahertz range. There is strong evidence to suggest that these behaviors do not depend on external feedback to the lasing ring from coupled output waveguides.

When considering the effect of conservative and dissipative scattering coefficients in a two-mode theoretical framework, good agreement has been found between the measured data and the model. Moreover, by means of a suitable fitting procedure, quantitative estimation of the otherwise unknown scattering parameters has been performed. The theoretical model shows that semiconductor ring cavities with no backscattering would operate in a complete unidirectional and bistable regime because of directional mode selection through cross-gain saturation. However, the backscattering strongly influences the lasing operation close to threshold where the bidirectional mode operation is observed. It appears that the dissipative scattering coefficient favors continuous-wave operation, either bidirectional or unidirectional, while the conservative scattering coefficient acts as a driving force for the alternate oscillations. Devices with deeper etched waveguides showed a direct transition from bidirectional continuous wave to unidirectional operating regime without exhibiting alternate oscillations. This behavior is in good agreement with the theory when assuming higher values of the scattering coefficients due to stronger interaction of the modes with the waveguide sidewall roughness. For even higher values of the scattering coefficients,

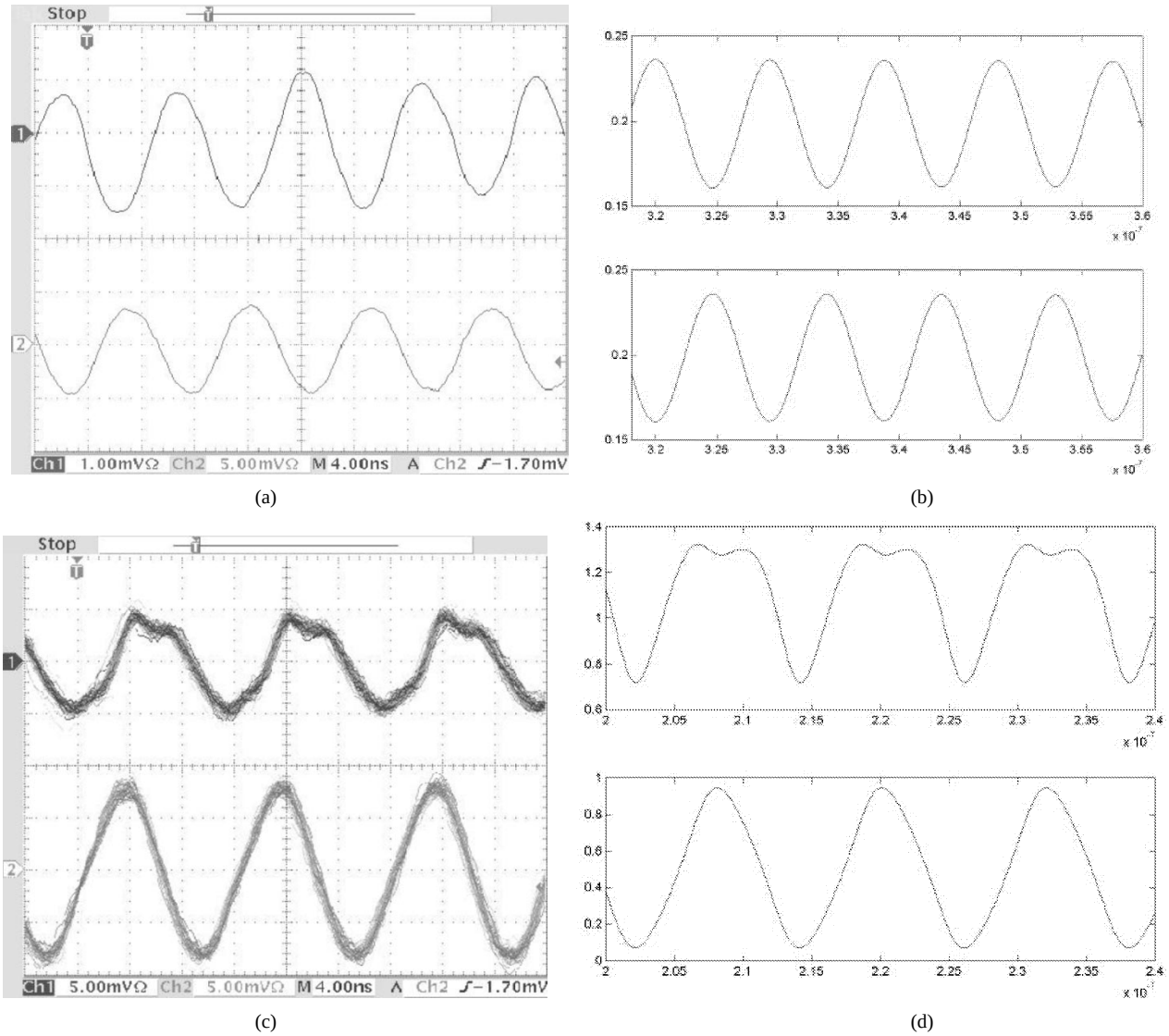

Fig. 7. Experimental and calculated waveforms of SRL mode intensities. (a) Experimental traces for the intensity of mode 1 (upper trace) and mode 2 (lower trace) for a ring current of 380 mA. (b) Calculated intensity waveforms for mode 1 (upper) and mode 2 (lower), for $\mu = 1.55$, that corresponds to a 380-mA ring current. (c) Experimental traces for the intensity of mode 1 (lower trace) and the photocurrent measured by in-line photodetector PD3 (upper trace) for a ring current of 440 mA. (d) Calculated waveforms for the intensity of mode 1 (lower) and the total intensity measured by in-line photodetector PD3 (upper), for $\mu = 2.15$, that corresponds to a 440-mA ring current. Time scales for calculated waveforms are in seconds.

complete bidirectional continuous wave operation is expected up to several times the threshold. Further investigations will be performed to assess the influence of the device geometry, the waveguide structure and the output coupler on the scattering coefficients. Unidirectional lasing in long-wavelength SRLs based on InP fabricated at Glasgow University, has also been observed, and it is expected that similar detailed operating characteristics will be found for these devices.

ACKNOWLEDGMENT

The authors are grateful to S. Balle and P. Mandel for helpful discussions and to A. Fanzio for technical support. The authors would also like to acknowledge the assistance given by the technical staff of the Nanoelectronics Research Centre and the Dry Etching Group in the Department of Electronics and Electrical Engineering, Glasgow University.

REFERENCES

[1] A. S. Liao and S. Wang, "Semiconductor injection lasers with a circular resonator," *Appl. Phys. Lett.*, vol. 36, pp. 801–803, 1980.
[2] T. F. Krauss, P. J. R. Laybourn, and J. S. Roberts, "CW operation of semiconductor ring lasers," *Electron. Lett.*, vol. 26, pp. 2095–2097, 1990.
[3] J. P. Hoimer, D. C. Craft, G. R. Hadley, and G. A. Vawter, "CW room temperature operation of y-junction semiconductor ring lasers," *Electron. Lett.*, vol. 28, pp. 374–375, 1992.
[4] G. Griffel, J. H. Abeles, R. J. Menna, A. M. Braun, J. C. Connolly, and M. King, "Low threshold InGaAsP ring lasers fabricated using bi-level dry etching," *IEEE Photon. Technol. Lett.*, vol. 12, pp. 146–148, 2000.
[5] J. P. Hoimer and G. A. Vawter, "Unidirectional semiconductor ring laser with racetrack cavities," *Appl. Phys. Lett.*, vol. 63, pp. 2457–2459, 1993.
[6] S. Oku, M. Okayasu, and M. Ikeda, "Low-threshold operation of square-shaped semiconductor ring lasers (orbiter lasers)," *IEEE Photon. Technol. Lett.*, vol. 3, pp. 588–590, 1991.
[7] H. Han, D. V. Forbes, and J. J. Coleman, "InGaAs-AlGaAs-GaAs strained-layer quantum-well heterostructure square ring lasers," *IEEE J. Quantum Electron.*, vol. 31, pp. 1994–1997, 1995.
[8] C. Ji, M. H. Leary, and J. M. Ballantyne, "Long-wavelength triangular ring laser," *IEEE Photon. Technol. Lett.*, vol. 9, pp. 1469–1471, 1997.

[9] T. F. Krauss, R. M. De La Rue, P. J. R. Laybourn, B. Vogele, and C. R. Stanley, "Efficient semiconductor ring lasers made by a simple self-aligned fabrication process," *IEEE J. Select. Topics Quantum Electron.*, vol. 1, pp. 757–761, 1995.
[10] T. M. Cockerill, D. V. Forbes, J. A. Dantzig, and J. J. Coleman, "A strained-layer InGaAs-GaAs-AlGaAs buried heterostructure quantum-well lasers by three-step selective area metalorganic chemical vapor deposition," *IEEE J. Quantum Electron.*, vol. 30, 1994.
[11] J. P. Zhang, D. Y. Chu, S. L. Wu, W. G. Bi, R. C. Tiberio, C. W. Tu, and S. T. Ho, "Directional light output from photonic-wire microcavity semiconductor lasers," *IEEE Photon. Technol. Lett.*, vol. 8, pp. 968–970, 1996.
[12] T. F. Krauss, R. M. De La Rue, and P. J. R. Laybourn, "Impact of output coupler configuration on operating characteristics of semiconductor ring lasers," *J. Lightwave Technol.*, vol. 13, pp. 1500–1507, 1995.
[13] R. van Roijen, E. C. Pennings, M. J. N. van Stralen, J. M. M. van der Heijden, T. van Dongen, and B. H. Verbeek, "Compact InP-based ring lasers employing multi-mode interference couplers and combiners," *Appl. Phys. Lett.*, vol. 64, pp. 1753–1755, 1994.
[14] J. J. Liang, S. T. Lau, M. H. Leary, and J. M. Ballantyne, "Unidirectional operation of waveguide diode ring lasers," *Appl. Phys. Lett.*, vol. 70, pp. 1192–1194, 1997.
[15] S. Oku, M. Okayasu, and M. Ikeda, "Control of unidirectional oscillations in semiconductor orbiter lasers," *IEEE Photon. Technol. Lett.*, vol. 3, pp. 1066–1068, 1991.
[16] M. Sorel, P. J. R. Laybourn, G. Giuliani, and S. Donati, "Unidirectional bistability in semiconductor waveguide ring lasers," *Appl. Phys. Lett.*, vol. 80, pp. 3051–3053, 2002.
[17] L. N. Menegozzi and W. E. Lamb, "Theory of a ring laser," *Phys. Rev. A*, vol. 8, pp. 2103–2125, 1973.
[18] C. L. O'Brian and M. Sargent III, "Theory of a multimode quasiequilibrium semiconductor laser," *Phys. Rev. A*, vol. 48, pp. 3071–3091, 1993.
[19] C. Etrich, P. Mandel, N. B. Abraham, and H. Zeghlache, "Dynamics of a two-mode semiconductor laser," *IEEE J. Quantum Electron.*, vol. 28, pp. 811–821, 1992.
[20] R. J. C. Spreew, R. Centeno Neelon, N. J. vanDruten, E. R. Eliel, and J. P. Woerdman, "Mode coupling in He-Ne ring laser with backscattering," *Phys. Rev. A*, vol. 4, pp. 4315–4324, 1990.
[21] F. C. Cheng, "Investigation of a dye ring laser with backscattering," *Phys. Rev. A*, vol. 45, pp. 5220–5227, 1992.
[22] M. Sorel, P. J. R. Laybourn, A. Scirè ;, S. Balle, G. Giuliani, R. Miglierina, and S. Donati, "Alternate oscillations in semiconductor ring laser," *Opt. Lett.*, vol. 27, pp. 1992–1994, 2002.
[23] S. E. Hicks, W. Parkes, J. A. H. Wilkinson, and C. D. W. Wilkinson, "Reflectance modeling for in situ dry etch monitoring of bulk SiO_2 and III-V multilayer structures," *J. Vac. Sci. Technol. B*, vol. 12, pp. 3306–3310, 1994.
[24] J. P. Hoimer and G. A. Vawter, "Passive mode locking of monolithic semiconductor ring lasers at 86 GHz," *Appl. Phys. Lett.*, vol. 63, pp. 1598–1600, 1993.
[25] G. Giuliani, P. Cinguino, and V. Seano, "Multifunctional characteristics of 1.5-μm two-section amplifier-modulator-detector SOA," *IEEE Photon. Technol. Lett.*, vol. 8, pp. 367–369, 1996.
[26] T. Numai, "Analysis of signal voltage in a semiconductor ring laser gyro," *IEEE J. Quantum Electron.*, vol. 36, pp. 1161–1167, 2000.
[27] H. A. Haus, H. Statz, and I. W. Smith, "Frequency locking of modes in a ring laser," *IEEE J. Quantum Electron.*, vol. QE-21, pp. 78–85, 1985.
[28] E. J. D'Angelo, E. Izaguirre, G. B. Mindlin, L. Gil, and J. R. Tredicce, "Spatiotemporal dynamics of lasers in the presence of an imperfect O(2) symmetry," *Phys. Rev. Lett*, vol. 68, pp. 3702–3704, 1992.
[29] H. Kawaguchi, *Bistabilities and Nonlinearities in Laser Diodes.* Norwood, MA: Artech House, 1994, p. 151.

M. Sorel (M'99) received the electronics engineering degree and the Ph.D. degree in electronics and computer science from the Università di Pavia, Pavia, Italy, in 1995 and 1999, respectively.

In 1998, he joined the Optoelectronics Group at the University of Glasgow, Glasgow, U.K., and he was recipient of a Marie-Curie fellowship in 1999 for research on integrated optical gyroscopes. In 2002, he was appointed to a lectureship in the Department of Electronics and Electrical Engineering, University of Glasgow. His research activities include interferometry, locking phenomena, semiconductor mode-locked lasers, and integrated semiconductor ring lasers.

G. Giuliani (M'99) was born in Milan, Italy, in 1969. He received the Ph.D. degree in electronics and computer science from the Università di Pavia, Pavia, Italy, in 1997.

Since 2000, he has been an Assistant Professor at the Università di Pavia. His research interests include semiconductor lasers, semiconductor optical amplifiers, optical amplifier noise, interferometry, and optoelectronic sensors.

A. Scirè (M'99) was born in Rimini, Italy, in 1971. He received the electronics engineering degree and the Ph.D. degree in electronics engineering and computer science from the University of Pavia, Pavia, Italy, in 1995, working in the Optoelectronics Group.

He is presently with the Instituto Mediterraneo de Estudios Avanzados (IMEDEA), Mallorca, Spain, as a recipient of a Marie Curie Fellowship from the European Community. His research interests include modelling of laser diodes and of active optical components, dynamics of vertical-cavity surface-emitting lasers (VCSELs) due to saturable absorption, VCSEL arrays, coupled vectorial oscillators, semiconductor ring lasers, and nonlinear dynamics in optically injected laser diodes. He is the author of 20 papers.

R. Miglierina (M'99) received the electronic engineering degree in 2001 from the University of Pavia, Pavia, Italy, where he is currently working toward the Ph.D. degree in the Optoelectronics Group, Electronics Department.

His research interests include experimental characterization and modelling of semiconductor devices, with particular attention to semiconductor ring lasers and high-bandwidth photodetectors.

S. Donati (M'75–SM'98–F'03) has been a Professor of Optoelectronics with the Department of Electronics, Faculty of Engineering, University of Pavia, Pavia, Italy, since 1980, where he has carried out research on photodetectors and noise, electro-optical instrumentation, and especially self-mixing interferometry, passive fiber-optic components, optical interconnection, optical chaos, and cryptography. He has authored or coauthored about 200 papers and one book, *Photodetectors* (Englewood Cliffs, NJ: Prentice Hall, 1999).

Dr. Donati is presently the LEOS Vice President of Region 8 Membership, Treasurer of the Italian LEOS Chapter, and Counselor of the IEEE Student Branch in Pavia. With T. Tambosso, he has promoted the International Workshop on Fiber Optics and Passive Components (WFOPC). He has also organized and chaired two editions of the Conference on Optical Distance Measurements and Applications (ODIMAP), held in 1999 and 2001. He founded (1996) and was the past Chairman (1997-2001) of the Italian LEOS Chapter. From 1986 to 1992, he was the Director of *Alta Frequenza*, a scientific review in electronics published by the Italian Association of Electronic Engineers (AEI). He was Chairman of the Italian Optoelectronics Society (1992-1995) of AEI.

P. J. R. Laybourn graduated in mechanical and electrical sciences at Cambridge University, Cambridge, U.K. He received the Ph.D. degree in microwave harmonic generation from Leeds University, Leeds, U.K.

In 1966, he joined the Embryo Optical Fibre Communications Group at the University of Southampton, Southampton, U.K. In 1971, he was appointed to a lectureship in the Department of Electronics and Electrical Engineering, University of Glasgow, Glasgow, U.K., where he now holds a Personal Chair of Electronic Engineering. He joined the Integrated Optics (now Optoelectronics) research group, where he has worked on ion-exchanged glass and lithium niobate guides and devices, waveguide lenses, and semiconductor ring lasers, filters, and gyroscopes.